

## SUPPORTING INFORMATION

### **Mechanism-Based Inactivation by Aromatization of the Transaminase BioA Involved in Biotin Biosynthesis in *Mycobacterium tuberculosis***

Ce Shi,<sup>a</sup> Todd W. Geders,<sup>b</sup> Sae Woong Park,<sup>c</sup> Daniel J. Wilson,<sup>a</sup> Helena I. Boshoff,<sup>d</sup> Abayomi, Orisadipe,<sup>d</sup> Clifton E. Barry III,<sup>d</sup> Dirk Schnappinger,<sup>c</sup> Barry C. Finzel,<sup>b</sup> Courtney C. Aldrich<sup>a\*</sup>

<sup>a</sup>Center for Drug Design, Academic Health Center, University of Minnesota, MN, 55455, United States

<sup>b</sup>Department of Medicinal Chemistry, University of Minnesota, MN, 55455, United States

<sup>c</sup>Department of Microbiology and Immunology, Weill Cornell Medical College, New York, NY, 10065, United States

<sup>d</sup>Tuberculosis Research Section, National Institute of Allergy and Infectious Diseases, Bethesda, MD, 20892, United States

\**email: aldri015@umn.edu*

## Table of Contents

I. Complete citation for reference #25.....	S3
II. Characterization data of key intermediates for compound <b>2</b> .....	S3
III. General description of transaminase assays.....	S4
IV Cell Cytotoxicity Assays .....	S5
V. MS/MS Analysis of PLP-inhibitor adduct.....	S6
VI. Co-crystal data of BioA-inhibitor.....	S7
VII. <sup>1</sup> H and <sup>13</sup> C NMR Spectra.....	S10

## I. Complete citation for Reference 25.

Adams, P. D.; Afonine, P. V.; Bunkóczi, G.; Chen, V. B.; Davis, I. W.; Echols, N.; Headd, J. J.; Hung, L. W.; Kapral, G. J.; Grosse-Kunstleve, R. W.; McCoy, A. J.; Moriarity, N. W.; Oeffner, R.; Read, R. J.; Richardson, D. C.; Richardson, J. S.; Terwilliger, T. C.; Zwart, P. H. *Acta Crystallogr. D Biol. Crystallogr.* **2010**, *66*, 213.

## II. Characterization data of key intermediates for compound 2

**(S)-N-[6-(tert-Butyldimethylsilyloxy)hex-1-en-3-yl]-2,2,2-trichloroacetamide (enan-11).** The title compound was prepared analogously to **11** but employing [(S)-COP-Cl]<sub>2</sub> and obtained in 88% yield:  $[\alpha]_{\text{D}}^{23} = +4.5$  (*c* 0.8, CH<sub>2</sub>Cl<sub>2</sub>); HRMS (ESI<sup>-</sup>): calcd for C<sub>14</sub>H<sub>25</sub>Cl<sub>3</sub>NO<sub>2</sub>Si [M - H]<sup>-</sup> 372.0726, found 372.0710 (error 4.3 ppm).

**(S)-6-(tert-Butyldimethylsilyloxy)hex-1-en-3-amine (enan-12).** The title compound was prepared analogously to **12** from **enan-11** and obtained in 71% yield:  $[\alpha]_{\text{D}}^{23} = +15$  (*c* 0.5, CH<sub>2</sub>Cl<sub>2</sub>); HRMS (ESI<sup>+</sup>): calcd for C<sub>12</sub>H<sub>28</sub>NOSi [M + H]<sup>+</sup> 230.1935, found 230.1936 (error 0.4 ppm).

**tert-Butyl ((R)-1-[(S)-6-(tert-butyldimethylsilyloxy)hex-1-en-3-yl]amino)-1-oxobut-3-en-2-yl)carbamate (enan-14).** The title compound was prepared analogously to **14** from **enan-12** and (*R*)-*N*-Boc-vinylglycine<sup>13c</sup> and obtained in 75% yield:  $[\alpha]_{\text{D}}^{23} = +7.8$  (*c* 3.7, CH<sub>2</sub>Cl<sub>2</sub>); HRMS (APCI<sup>+</sup>): calcd for C<sub>21</sub>H<sub>41</sub>N<sub>2</sub>O<sub>4</sub>Si [M + H]<sup>+</sup> 413.2830, found 413.2838 (error 1.9 ppm).

**tert-Butyl {(3*R*, 6*S*)-6-[3-(tert-butyldimethylsilyloxy)propyl]-2-oxo-3,6-dihydropyridin-3-nonyl}carbamate (enan-15).** The title compound was prepared analogously to **15** from **enan-14** and obtained in 88% yield: mp 107–108 °C;  $[\alpha]_{\text{D}}^{23} = -24$  (*c* 0.28, CH<sub>2</sub>Cl<sub>2</sub>); HRMS (APCI<sup>+</sup>): calcd for C<sub>19</sub>H<sub>37</sub>N<sub>2</sub>O<sub>4</sub>Si [M + H]<sup>+</sup> 385.2517, found 385.2520 (error 0.8 ppm).

**tert-Butyl [(3*R*, 6*S*)-6-(3-hydroxypropyl)-2-oxo-3,6-dihydropyridin-3-nonyl]carbamate (enan-S3).** The title compound was prepared analogously to **S3** from **enan-15** and obtained in 70% yield:  $[\alpha]_{\text{D}}^{23} = -7.8$  (*c* 0.9, CH<sub>2</sub>Cl<sub>2</sub>); HRMS (APCI+): calcd for C<sub>13</sub>H<sub>23</sub>N<sub>2</sub>O<sub>4</sub> [M + H]<sup>+</sup> 271.1652, found 271.1655 (error 1.1 ppm).

**(3*R*, 6*S*)-3-Amino-6-(3-hydroxypropyl)-3,6-dihydropyridin-2(3*H*)-one hydrochloride salt (2).** The title compound was prepared analogously to **1** from **enan-S3** and obtained in 80% yield: mp 184–185 °C;  $[\alpha]_{\text{D}}^{23} = +34$  (*c* 0.5, MeOH); HRMS (ESI+): calcd for C<sub>8</sub>H<sub>15</sub>N<sub>2</sub>O<sub>2</sub> [M + H]<sup>+</sup> 171.1128, found 171.1128 (error 0 ppm).

### III. Transaminase Assays with Alanine Aminotransferase and Aspartate Aminotransferase.

In order to assess potential off target activity of **1** alanine aminotransferase (glutamic-pyruvic transaminase, SIGMA-ALDRICH catalogue# G8255) and aspartate aminotransferase (glutamic-oxalacetic transaminase, SIGMA-ALDRICH catalogue# G2751) were evaluated. Enzyme activity could be followed by measuring the consumption of NADH at A340 using the coupled enzyme system described by the manufacturer (Sigma). In the case of glutamic-pyruvic transaminase, enzyme at 38 μM was incubated with 0.0625 – 1 mM **1** for 0, 5, 10, 20, 30 and 60 minutes. Enzyme inhibitor solutions were diluted 50-fold into reaction buffer (60 mM bicine pH 8.0, 0.2 mM alanine, 10 mM α-ketoglutarate, 0.1 mM NADH and 1.2 U lactic dehydrogenase) and the residual activity was measured by the consumption of NADH at A340. The data was analyzed by linear regression analysis ( $r^2 > 0.99$ ) and the slope provided the  $k_{\text{inact}}/K_{\text{I}}$ . Glutamic-oxalacetic transaminase was assayed by combining 10 nM enzyme, 100 mM bicine pH 8.0, 1 mM **1** and 0.13 mM PLP and allowing the mixture to incubate at ambient temperature for 30 minutes. The enzyme inhibitor mix was diluted 1.3 times in 5 mM aspartate, 5 mM α-ketoglutarate, 0.1 mM NADH and 0.9 U malic dehydrogenase. No inhibition was observed.

#### IV. Cell Cytotoxicity Assay

African green monkey *Cercopithecus aethiops* kidney cells (Vero, ATCC) were maintained in minimum essential medium (MEM) supplemented with 5% fetal bovine serum (FBS), 100 IU/mL penicillin and 100 µg/mL streptomycin. CHO-K1 cells (ATCC) were maintained in BD Select CHO medium (BD Biosciences) supplemented with 4 mM L-glutamine and pluronic F-68. Stock solutions of Inhibitor **1** in DMSO were added to the MEM media to afford the master mixes, yielding 0.5% DMSO and the final compound concentrations of 0.1, 0.5, 1.0 mM. Aliquots (200 µL) of the master mixes were plated in 96-well plates at  $2.0 - 3.0 \times 10^4$  cells per well for Vero cells and  $5.0 \times 10^5$  for CHO-K1 cells. Control wells contained either 0.5% DMSO (negative control) or 50% DMSO (positive control) and all reactions were done in triplicate. The plates were incubated for 72 h at 37 °C in a 5% CO<sub>2</sub>/95% air humidified atmosphere. Measurement of cell viability was carried out using a modified method of Mosmann based on 3-(4,5-dimethylthiazol-2-yl)-2,5-diphenyltetrazolium bromide (MTT).<sup>1</sup> MTT was prepared fresh at 1 mg/mL in serum-free, phenol red-free RPMI 1640 media. MTT solution (200 µL) was added to each well and the plate was incubated as described above for 3 h. The MTT solution was removed and the formazan crystals were solubilized with isopropanol (200 µL). The plate was read on a M5e spectrophotometer (Molecular Devices) at 570 nm for formazan and 650 nm for background subtraction. Cell viability was estimated as the percentage absorbance of sample relative to the DMSO control.

## V. MS/MS Analysis of PLP-inhibitor adduct

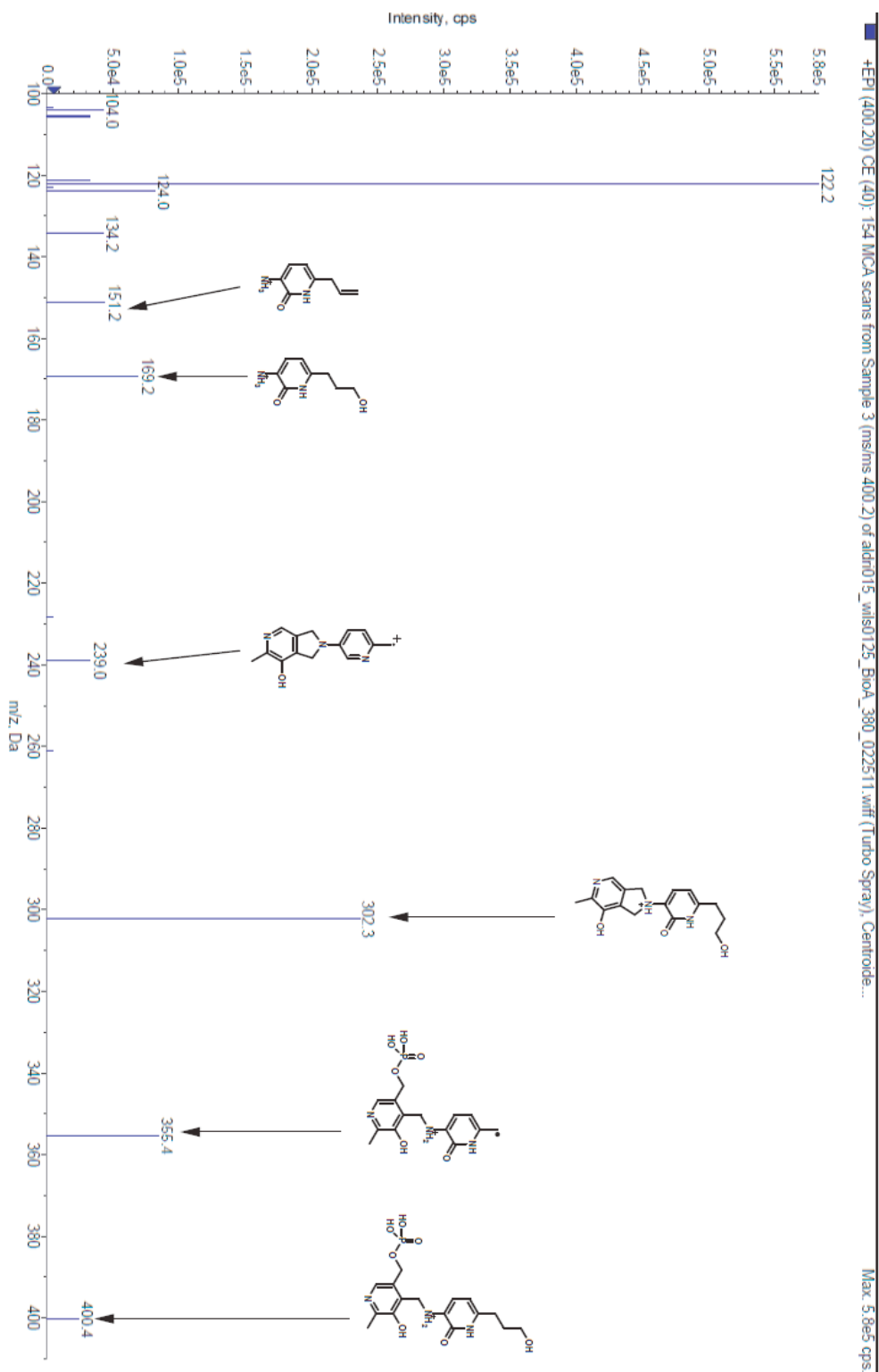


**Figure S1.** ESI MS/MS spectrum of molecular ion  $m/z$  400.4.

## VI. Co-crystal data of BioA-inhibitor

**Table S1.** Data collection and refinement statistics

	<i>3TFT, pre-reaction</i>	<i>3TFU, post-reaction</i>
<b>Data collection</b>		
Space group	P2 <sub>1</sub> 2 <sub>1</sub> 2 <sub>1</sub>	P2 <sub>1</sub> 2 <sub>1</sub> 2 <sub>1</sub>
Cell dimensions		
<i>a, b, c</i> (Å)	63.1, 66.4, 203.1	62.6, 66.3, 201.3
<i>a, b, g</i> (°)	90, 90, 90	90, 90, 90
Resolution (Å) <sup>a</sup>	40.3 – 1.95 (2.02 – 1.95)	39.2 – 1.94 (2.00 – 1.94)
<i>R</i> <sub>merge</sub> <sup>a,b</sup>	0.067 (0.116)	0.070 (0.154)
<i>I</i> / <i>sI</i> <sup>a</sup>	19.9 (11.9)	17.6 (7.8)
Completeness (%) <sup>a</sup>	99.2 (100)	98.2 (99.5)
Redundancy <sup>a</sup>	7.16 (7.22)	6.66 (6.49)
<b>Refinement</b>		
Resolution (Å)	40.3 – 1.95	39.2 – 1.94
No. reflections	62,631	62,293
<i>R</i> <sub>work</sub> / <i>R</i> <sub>free</sub> <sup>c,d</sup>	15.8/19.7	18.2/21.4
No. atoms		
Protein	6,383	6,258
Ligands	34	58
Water	822	701
<i>B</i> -factors		
Protein	19.7	23.0
Ligand/ion	15.5	27.8
Water	31.5	34.5
Wilson B	17.7	20.2
Ramachandran plot <sup>e</sup>		
Favored	97.5%	97.5%
Allowed	2.0%	2.3%
Disallowed	0.5%	0.2%
R.m.s. deviations		
Bond lengths (Å)	0.007	0.003
Bond angles (°)	1.050	0.836

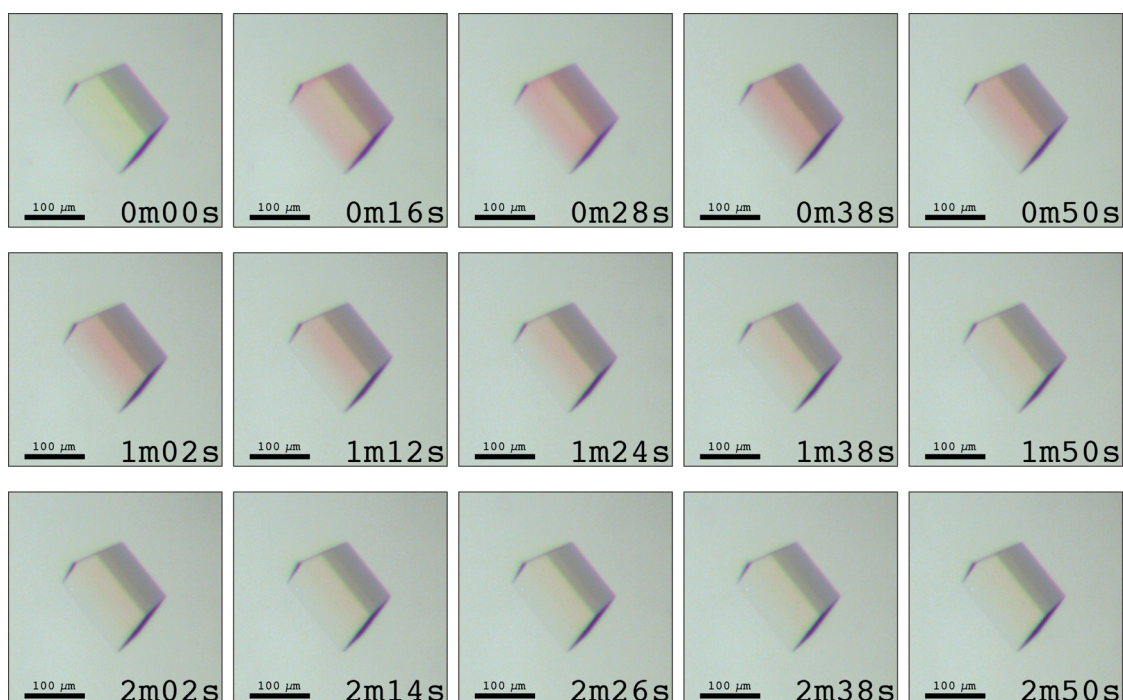
<sup>a</sup>Values in parenthesis are for outer shell

<sup>b</sup> $R_{merge} = \sum |I_i - \langle I \rangle| / \sum I_i$ , where  $I_i$  is the intensity of the  $i$ th observation and  $\langle I \rangle$  is the mean intensity

$^cR = \sum |F_O - F_C| / \sum |F_O|$  where  $F_O$  is the observed structure factor and  $F_C$  is the calculated structure factor used in the refinement

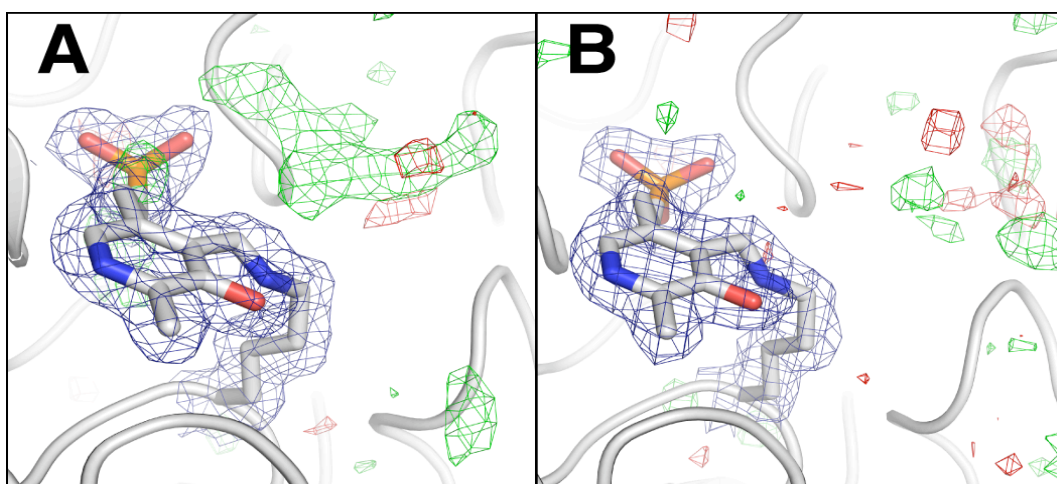
$^dR_{\text{free}} = \sum |F_O - F_C| / \sum |F_O|$  where  $F_O$  is the observed structure factor and  $F_C$  is the calculated structure factor from 5% of reflections not used in the refinement

<sup>e</sup>From output of MOLProbity

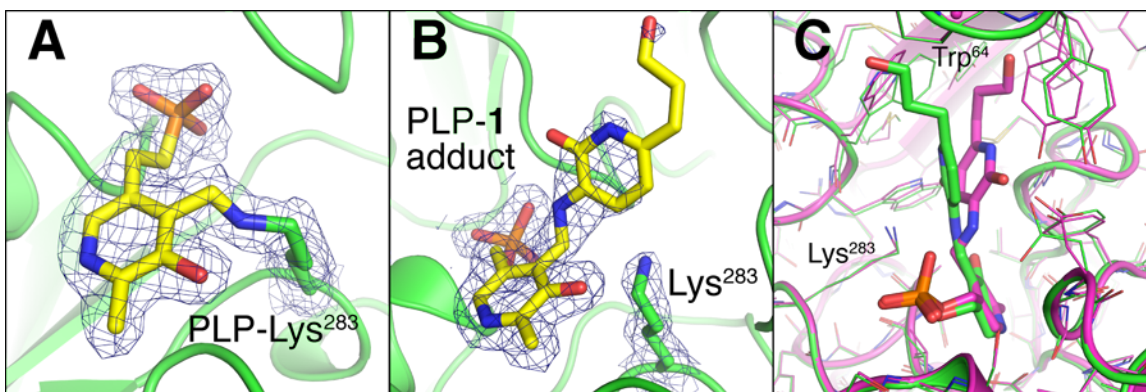


**Figure S2.** Still images from adding 0.5  $\mu\text{L}$  of reservoir solution containing 2 mM of compound **1** to a 1.5  $\mu\text{L}$  drop containing a yellow, PLP-loaded BioA crystal. The reddish **1** quickly concentrates within the crystal and then the crystal slowly turns colorless as **1** reacts with the PLP. The pre-reaction structure is from a maximally red-colored crystal (similar to the 28s image). The post-reaction structure is from a colorless crystal (similar to the 2m50s image).

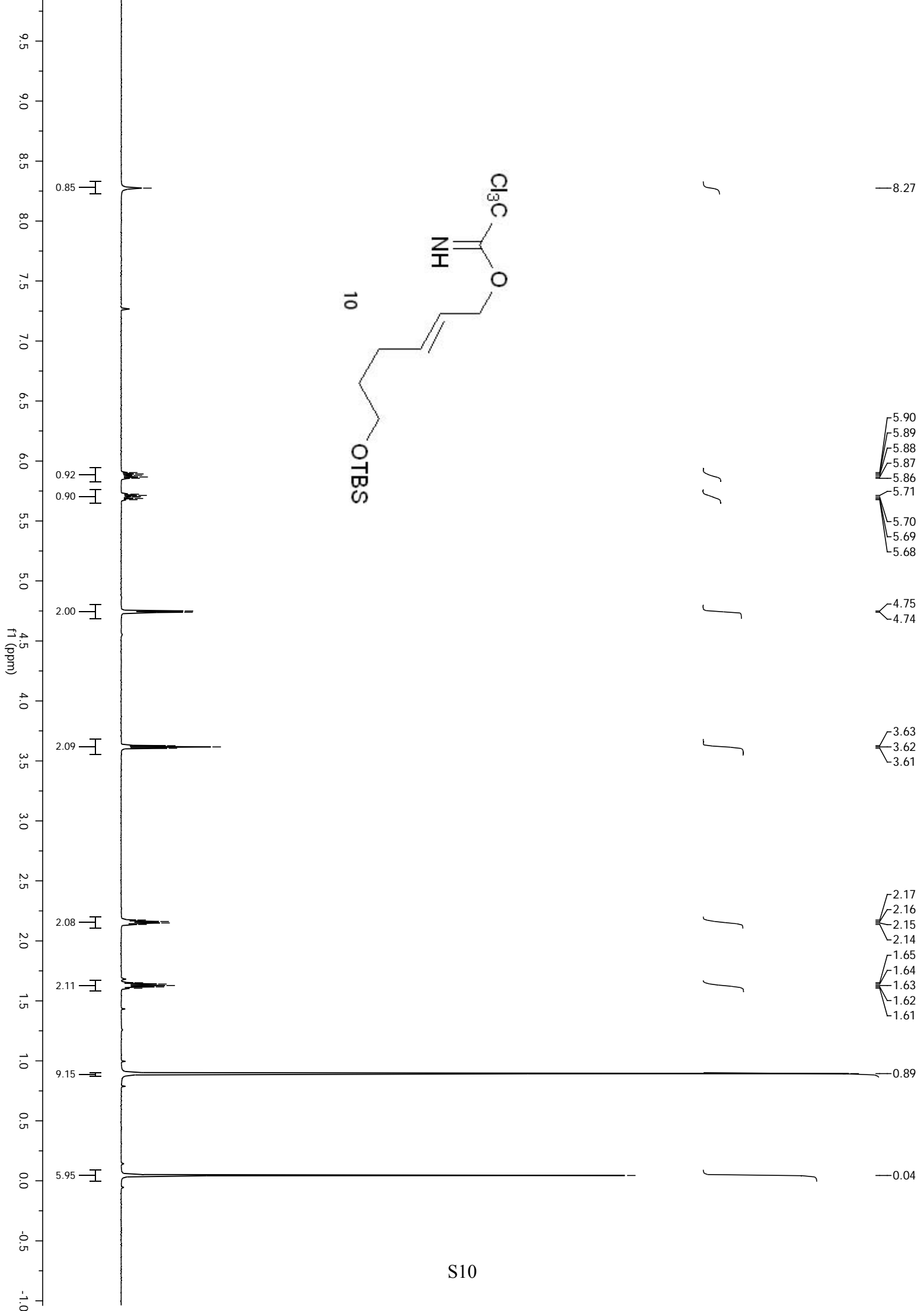


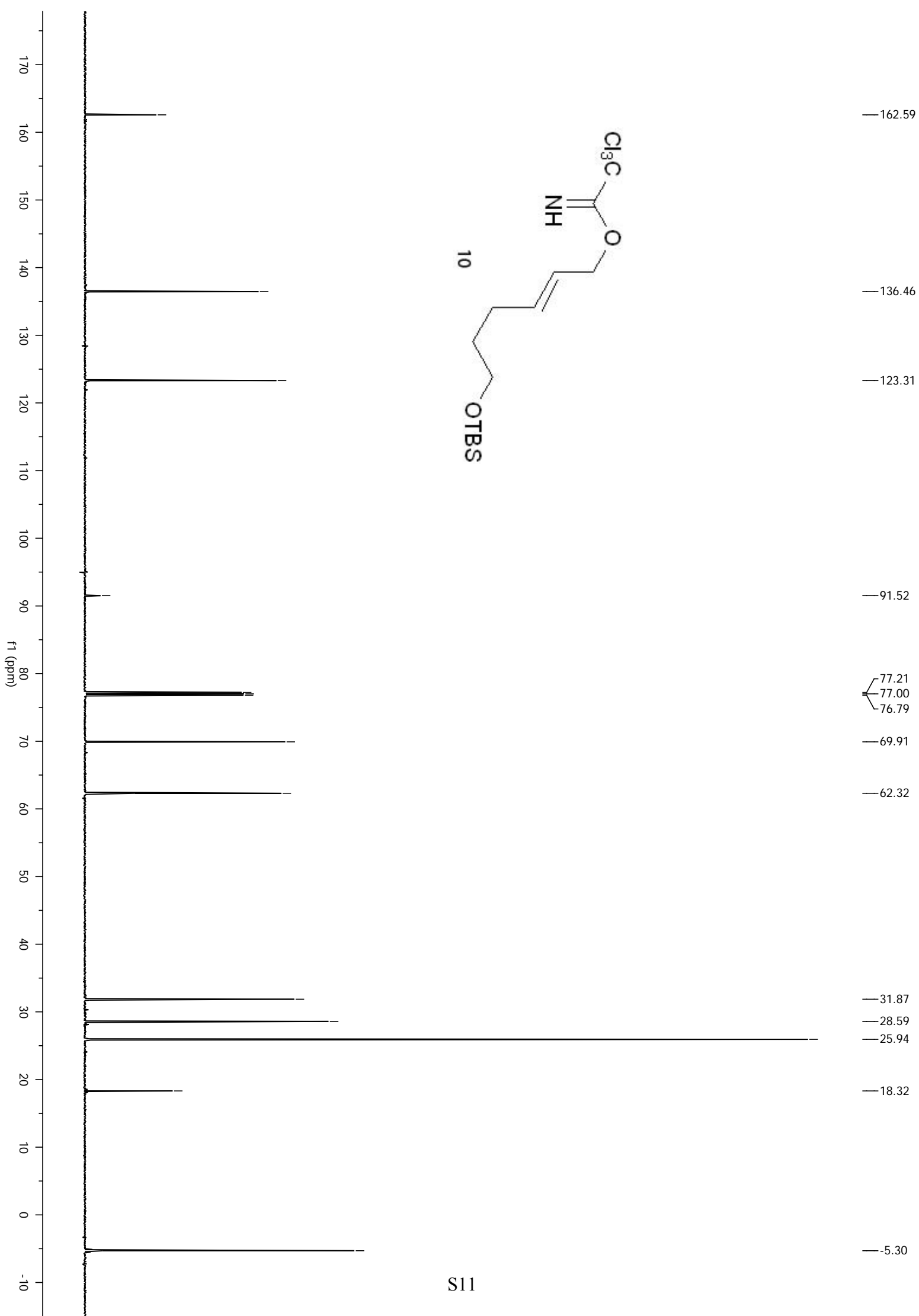


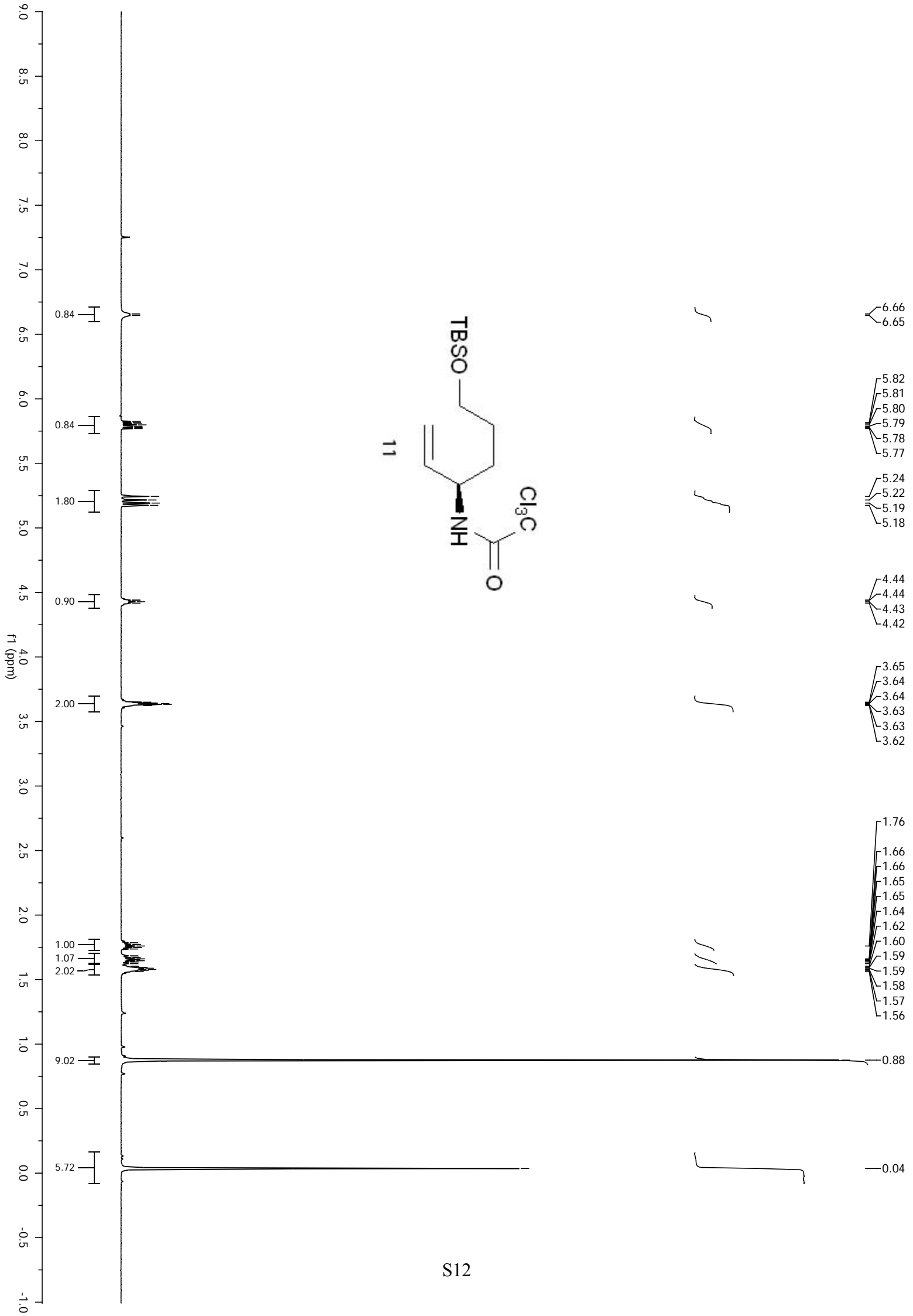
**Figure S3.** Final  $2F_o - F_c$  electron density contoured at 1.0 s (blue mesh) and  $F_o - F_c$  difference density contoured at +3 s (green mesh) and -3 s (red mesh) for the first molecule in the asymmetric unit (A) showing new positive difference density seen only in red crystals of BioA soaked with **1** for short periods of time (3-5 seconds). This large difference density is not observed in the second molecule in the asymmetric unit (B). Compound **1** could not be unambiguously modeled within this electron density, suggesting **1** binds in multiple conformations or had incomplete occupancy at this time point.

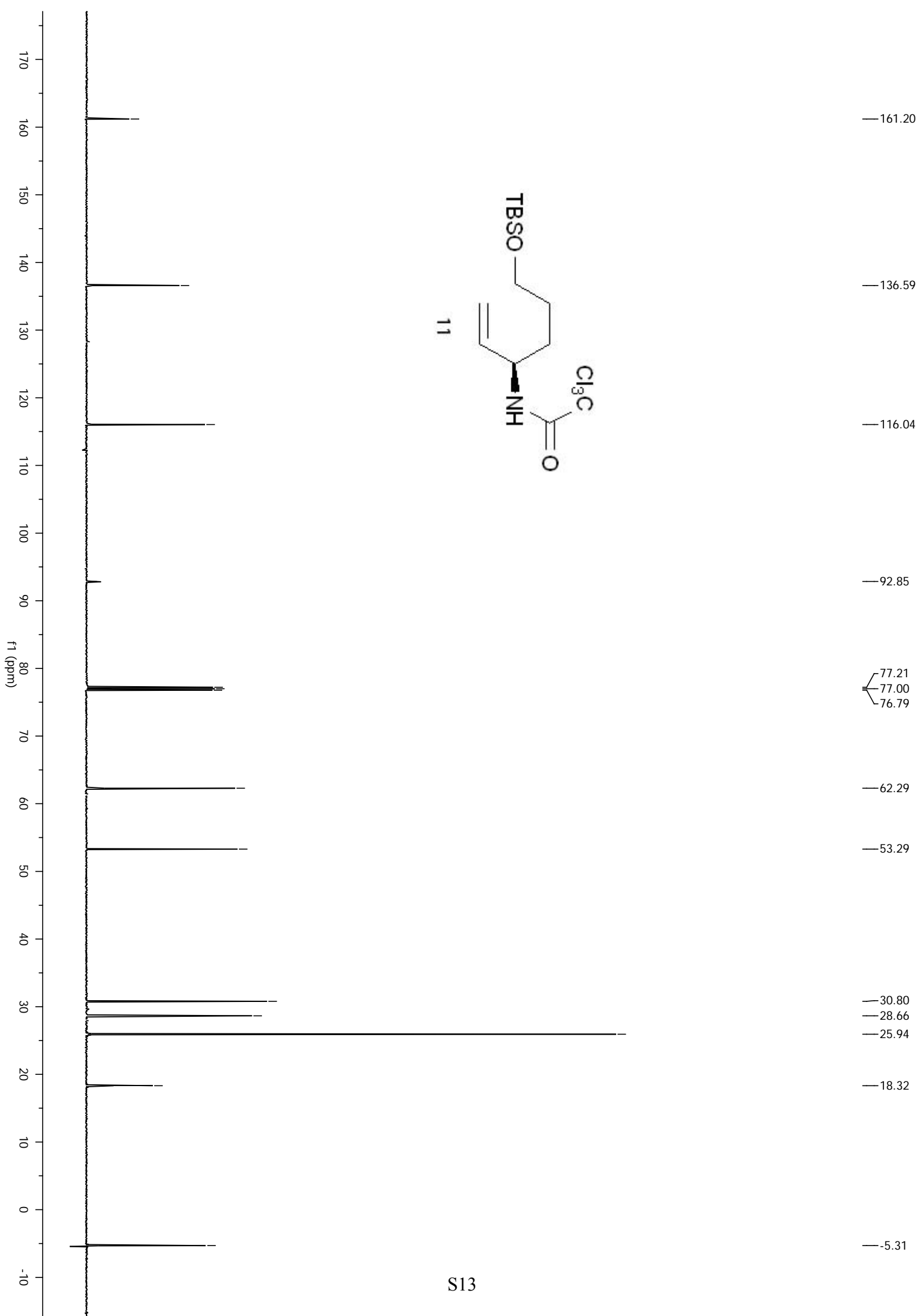
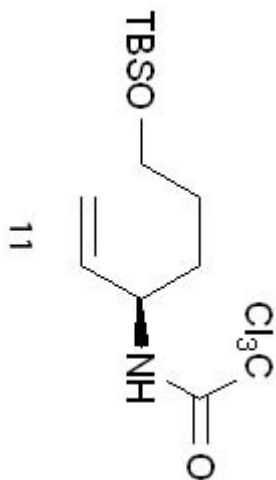


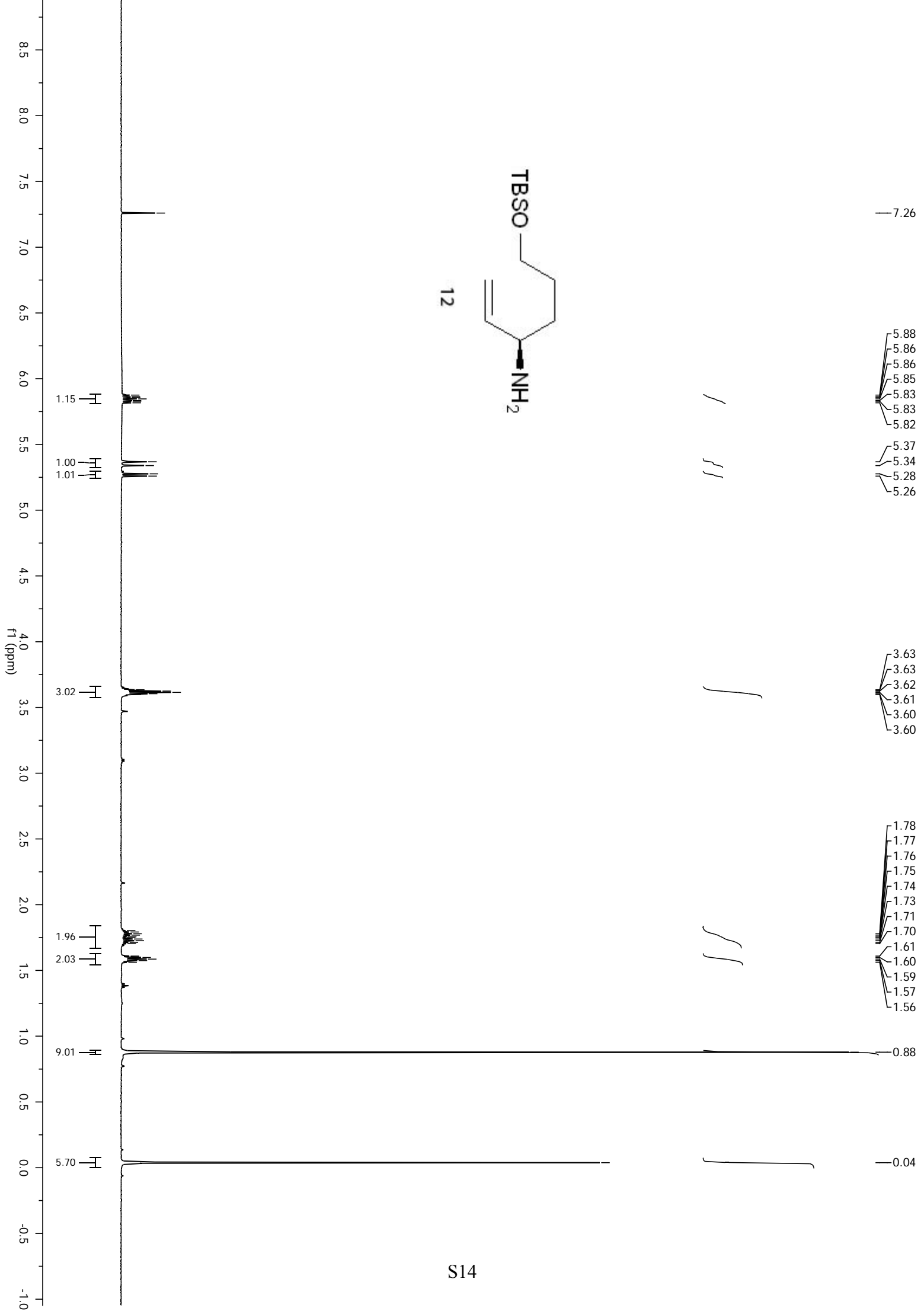
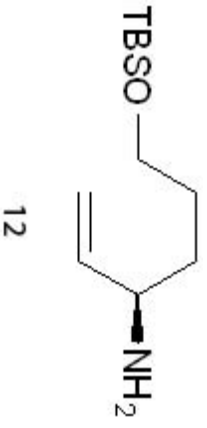
**Figure S4.** Final  $2F_o - F_c$  electron density contoured at 1.0 s (blue mesh) for the second molecule in the asymmetric unit for the pre-reaction (A) and post-reaction (B) structures. The first molecule in the asymmetric unit for each structure is shown in Figure 6 of main text. Although density was poorer for the PLP-1 adduct in the second molecule, there was still strong, continuous density leading from 4-position of the PLP ring. (C) An overlay of the first (green carbons) and second (magenta carbons) molecule in the asymmetric unit showing the conformation of the adduct is slightly different due to the position of Trp<sup>64</sup>.

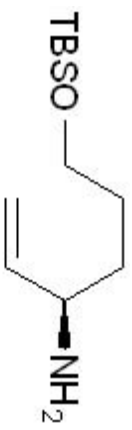




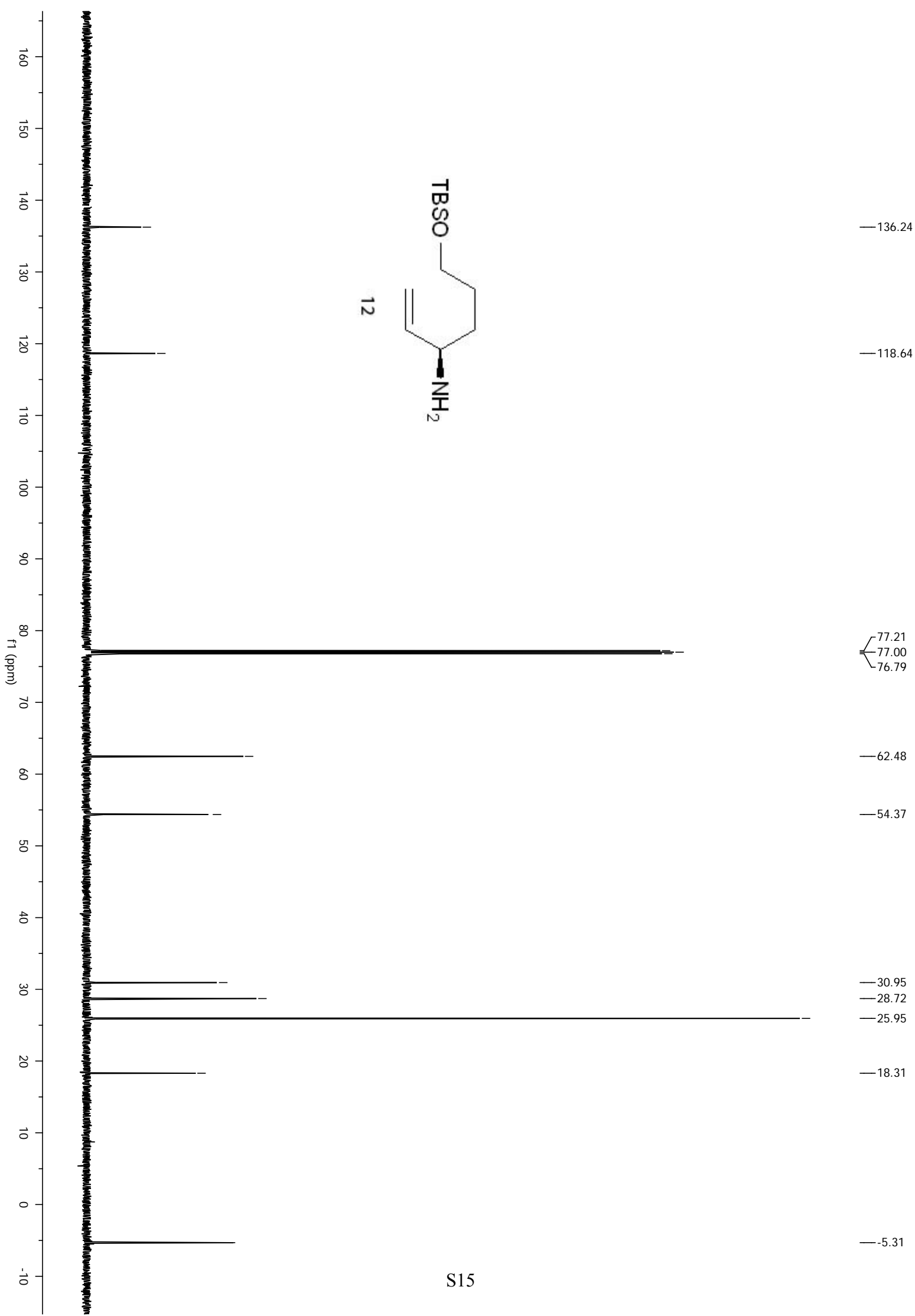


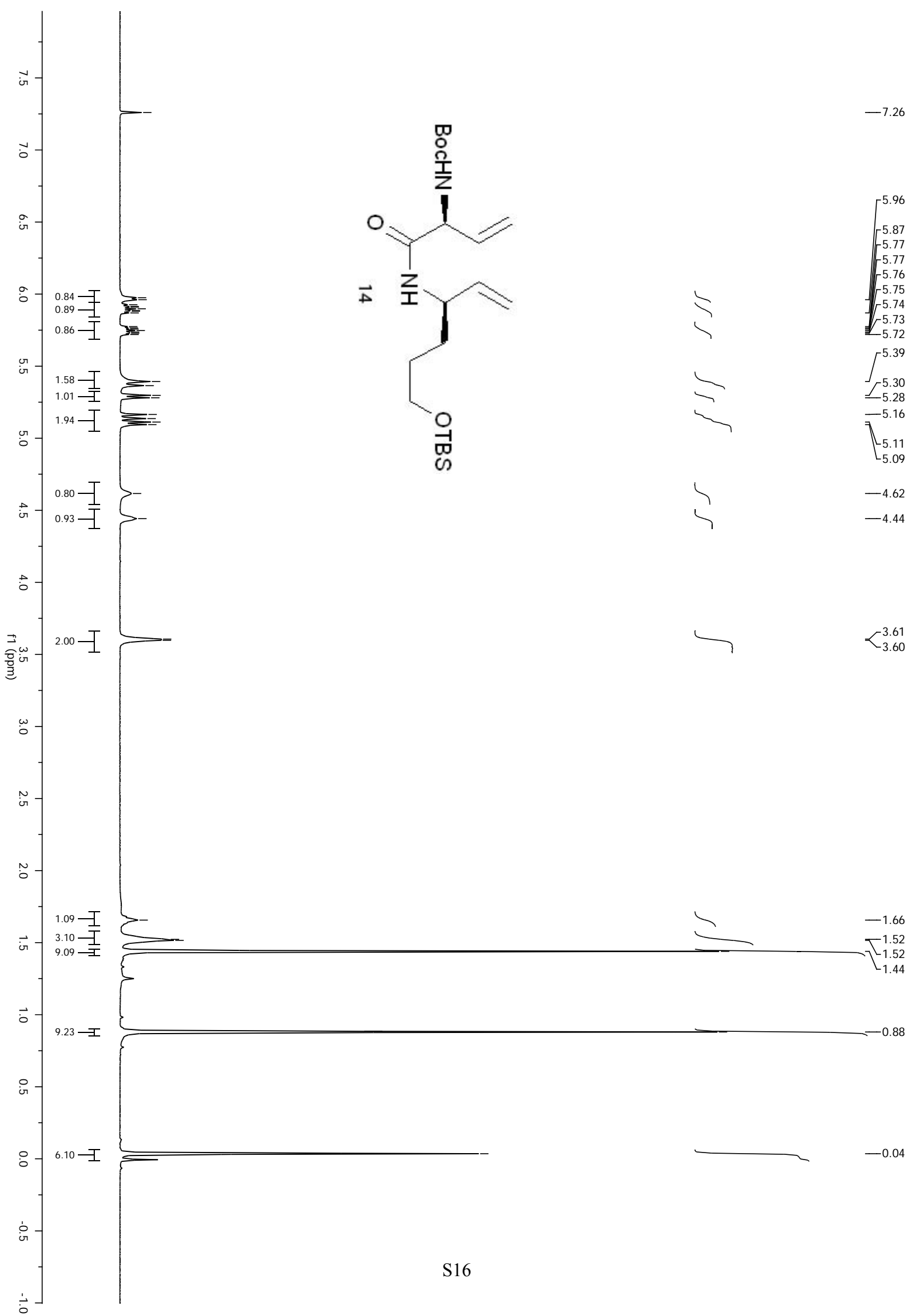




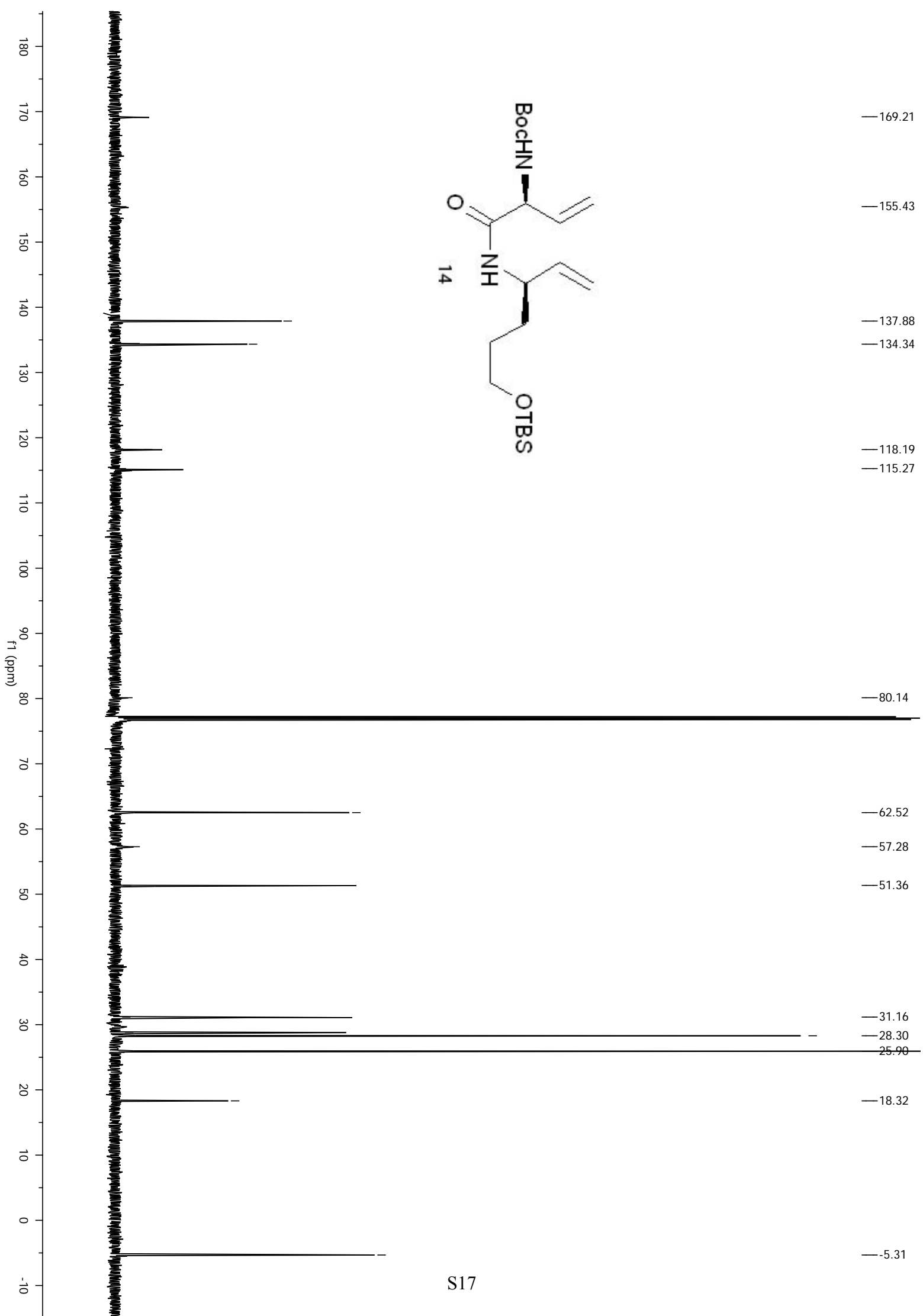


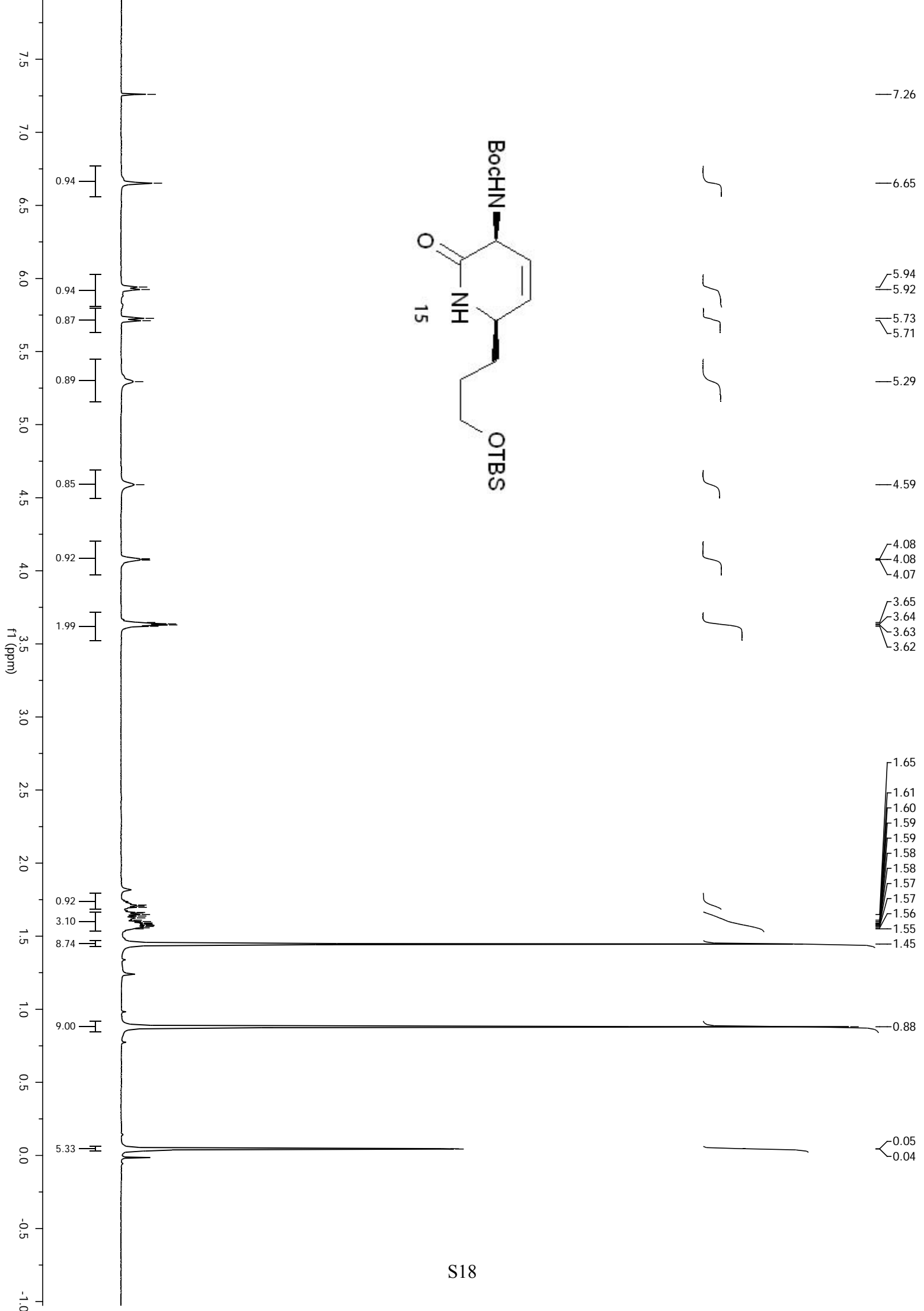
12

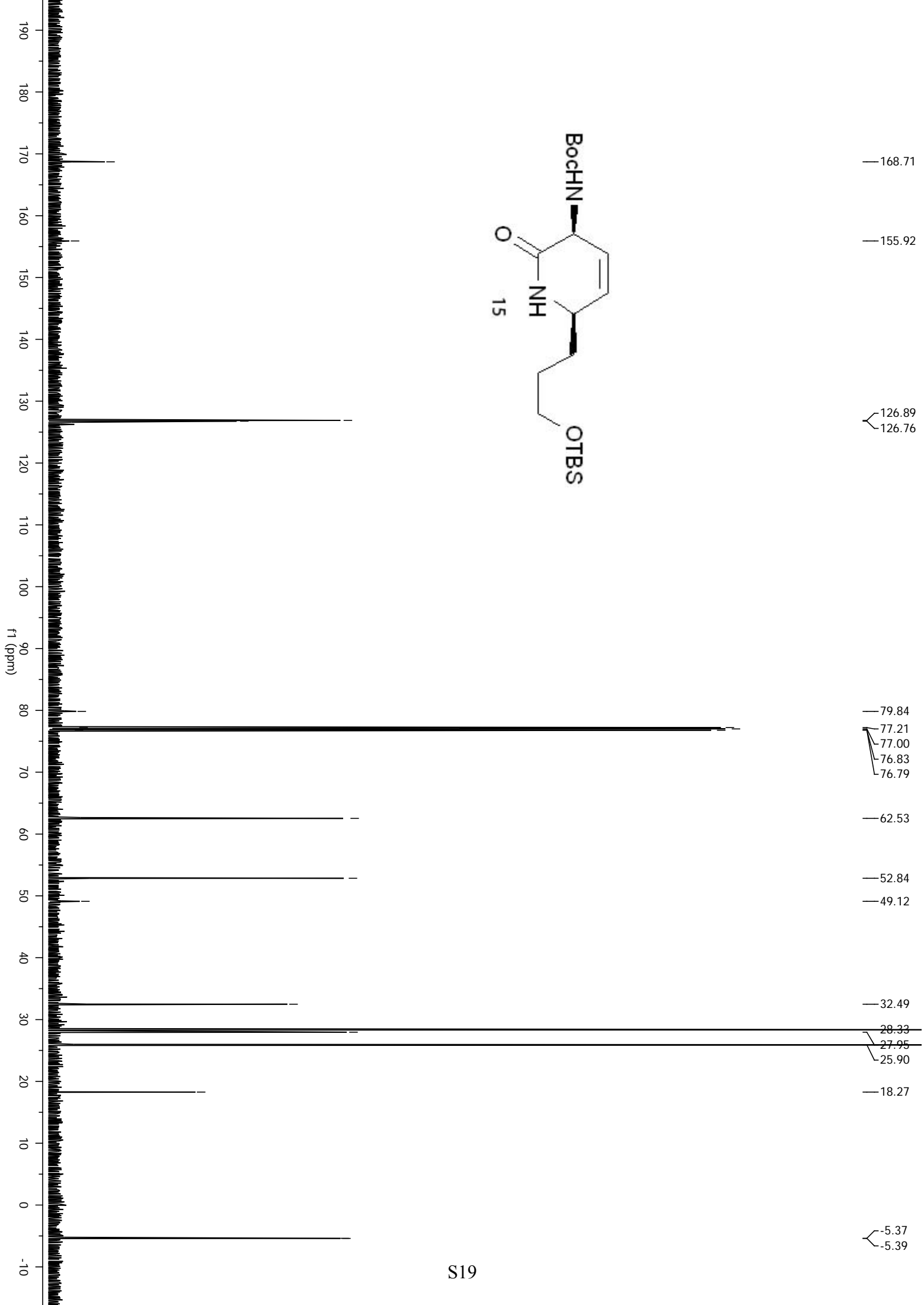


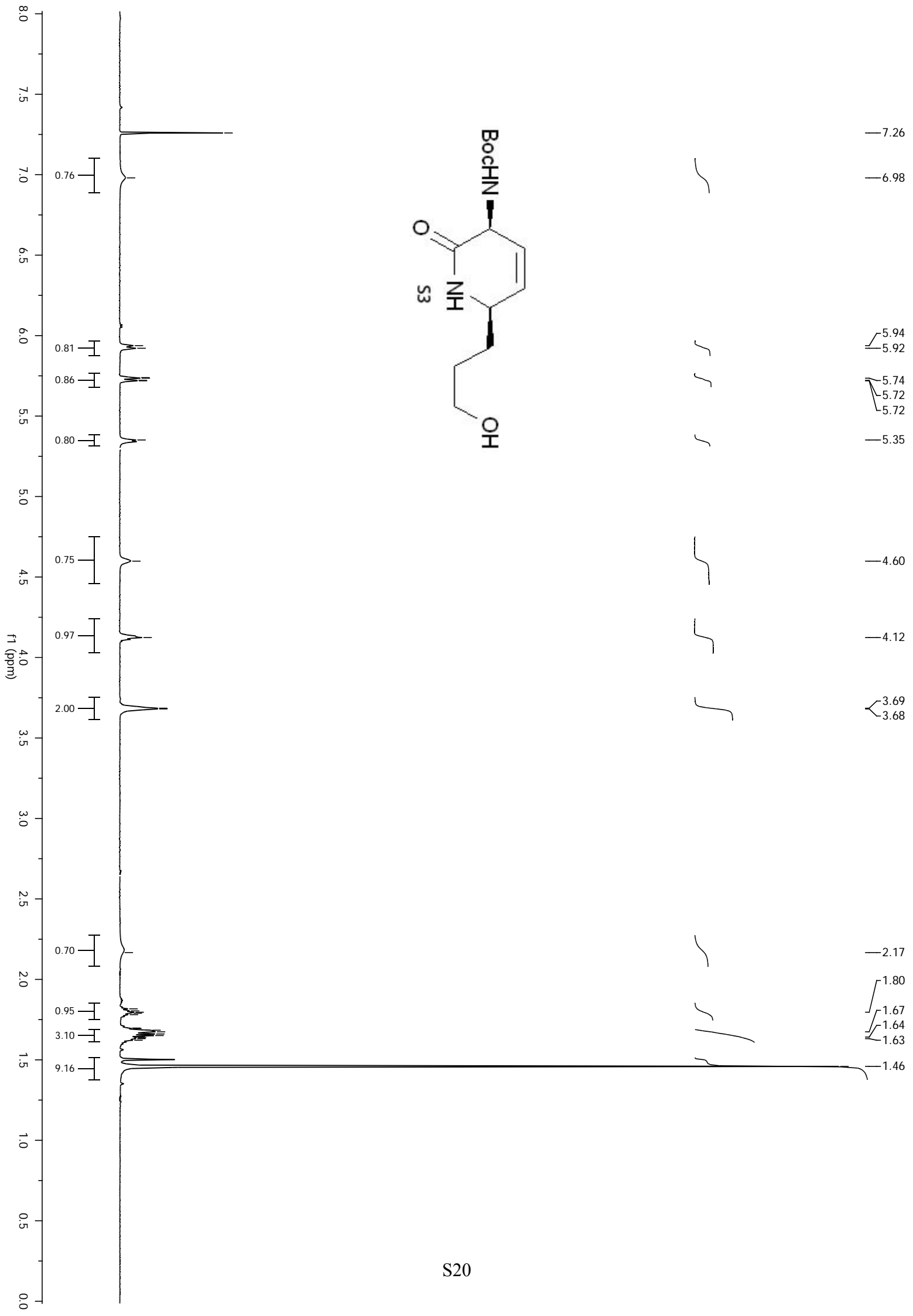


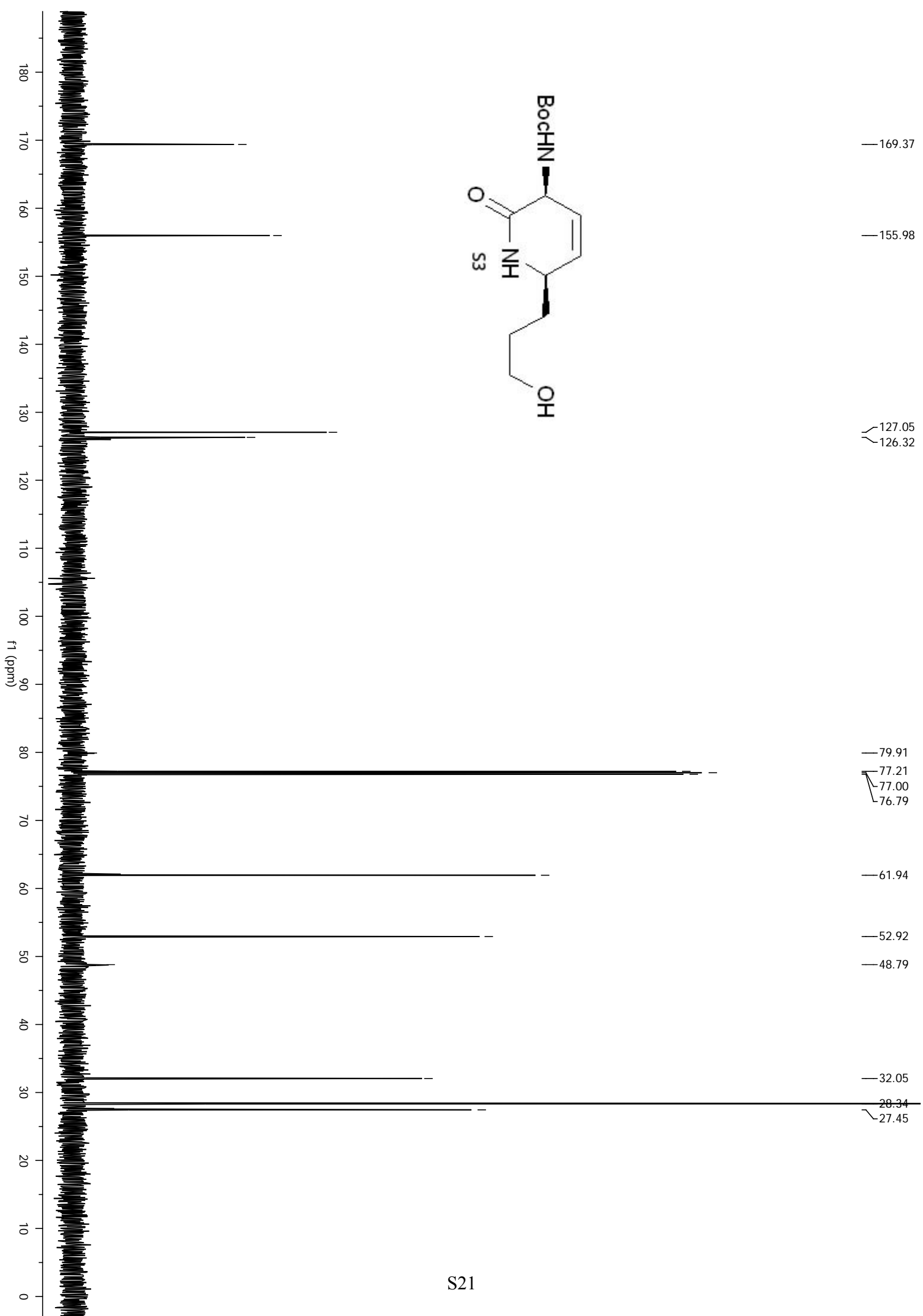












S21

